FULL PAPER

A Dual-Functional Persistently Luminescent Nanocomposite Enables Engineering of Mesenchymal Stem Cells for Homing and Gene Therapy of Glioblastoma

*Shu-Qi Wu, Cheng-Xiong Yang, and Xiu-Ping Yan**

Therapeutically engineered mesenchymal stem cells (MSC) have shown promising capability for glioblastoma (GBM) therapy; however, simultaneous tracking of their migration and long-term fate is urgently needed for clinical application. This study shows the design and fabrication of a dual-functional persistent luminescence nanocomposite (LPLNP-PPT/TRAIL) for effective therapeutic engineering and tracking of MSC in the meantime. LPLNP-PPT/TRAIL shows low-toxicity, near-infrared persistent luminescence emitting without in situ excitation, and superior in vivo deep brain tissue imaging, which can efficiently track the tumortropic migration of the therapeutic engineered MSC. Both in vitro and in vivo findings demonstrate the feasibility of LPLNP-PPT/TRAIL engineered MSC for inducing apoptosis of glioblastoma cells. This work first establishes an LPLNP-based dual-functional platform for cell engineering and provides us implications for GBM-related diagnosis and therapy.

1. Introduction

Glioblastoma (GBM) is the most lethal and aggressive brain tumor with a very poor prognosis.[1,2] Although surgical tumor resection combined with chemotherapy and radiation therapy has been used, the median survival of GBM patients is still limited to 14 months after initial diagnosis. The treatment resistance to common therapeutic agents causes recurrent tumor growth and brings severe challenges for clinical GBM therapy.[3] Gene therapy, which uses suicidal genes or gene-expressed therapeutic products to cure or inhibit diseases, has been considered as an alternative to traditional treatments for decades.[4] The main crucial challenges for in vivo gene-based GBM therapy are the blood–brain barrier and less tumor-targeting efficiency which limit the accumulation of therapeutic concentrations in GBM. To date, many nonviral vehicles or viral vectors have been developed to enhance therapeutic gene delivery.[5–7] However, only a low therapeutic efficiency can be typically achieved before the tumor-targeting capacity of vehicles is improved.

Mesenchymal stem cells (MSC) are attractive biologic carriers for delivering therapeutic agents into tumors due to their nature high tumor affinity.[8,9] Human tumor necrosis factor-related apoptosis-inducing ligand (TRAIL) is one particular tumor-specific protein inducing apoptosis and suppresses progression in a wide variety of GBM cells via interaction with the death receptors (DR)4/5.[10–12] MSC transduced with viral vectors to express TRAIL shows privileged tumor tropic nature and efficiently induces apoptosis in multiple GBM cell lines both in vitro and in vivo, so MSC-based gene therapy holds great potential for clinical applications.[13–15] For practical application, it is of crucial importance to propose a reliable noninvasive imaging approach to track the homing and migration of the therapeutic MSC in deep brain tissue.[16]

Optical imaging shows enormous advantages for cell tracking such as high sensitivity, high throughputs, nonradioactive, noninvasive, easy to operate, and cost-effective compared with common used magnetic resonance imaging or X-ray computed tomography imaging.[17] Common genetic transfection with optical reporters is limited by complex steps for gene modification and transfection while labeling with conventional fluorescent nanoparticles or organic dyes suffer from significant background autofluorescence interference with in situ excitation. Long persistent luminescence nanoparticles (LPLNP) show near-infrared (NIR)-persistent luminescence with long afterglow time and renewability by red light-emitting diode (LED) light.[18] Therefore, LPLNP has received great interest for cell imaging. Surface-modified LPLNP has shown to track RAW (murine macropgage) cells[19] and adipose-derived stem cells[20] with high signal-to-noise ratio. This suggests that the integration of LPLNP with therapeutic genes can highly enrich their functionalities for tracking and therapeutically engineering MSC.

Herein, we report the fabrication of dual-functional LPLNP engineered MSC for homing and gene therapy of GBM. LPLNP was coated with polyetherimide (PEI), polyethylene glycol (PEG), and transactivator of transcription (TAT) penetration peptide sequentially to obtain LPLNP-PPT core–shell nanocomposite (PPT refers to PEI-PEG-TAT). Further conjugation

S.-Q. Wu, Dr. C.-X. Yang, Prof. X.-P. Yan
Research Center for Analytical Sciences
Tianjin Key Laboratory of
Molecular Recognition and Biosensing
State Key Laboratory of Medicinal Chemical Biology
College of Chemistry
Nankai University
Tianjin 300071, China
E-mail: xpyan@nankai.edu.cn
Prof. X.-P. Yan
Collaborative Innovation Center of
Chemical Science and Engineering (Tianjin)
Tianjin 300071, China

DOI: 10.1002/adfm.201604992

was made with therapeutic plasmid genes (enhanced green fluorescence protein (EGFP)-TRAIL) to obtain LPLNP-PPT/TRAIL nanocomposite. The developed nanocomposite not only efficiently transfects MSC to express therapeutic TRAIL ligand without affecting their proliferation, differentiation, and tumor-homing abilities, but also effectively tracks the long-term migration of MSC in deep GBM model without any need for continuous external excitation. The engineered therapeutic and diagnostic MSC can be used as a novel type of theranostic reagents in GBM-related biomedicine.

2. Results and Discussion

2.1. Design, Preparation, and Characterization of LPLNP-PPT/TRAIL Composite

The NIR-emitting LPLNP was synthesized according to a previous procedure.[20] In order to achieve efficient plasmid DNA binding, high positively charged PEI[21,22] was used to adsorb negatively charged DNA. To guarantee the stability and the high amount of PEI coating, chemically active iodine groups were attached to LPLNP to obtain LPLNP-I. PEI coating was then conducted through substitution reaction of the amine of PEI and the iodine of LPLNP-I. The obtained LPLNP-PEI was PEGylated for the subsequent conjugation of TAT penetration peptide to enhance the cellular uptake and biocompatibility.[23] PEG was coated via amide condensation reaction while TAT peptide was conducted through specific addition reaction of the mercapto of cysteine on TAT peptide and the maleimide of the bonded PEG (**Figure 1**A). After sequential surface modification of PEI, PEG, and TAT, the synthesized LPLNP-PPT has an obvious core–shell nanostructure with a shell thickness of 2.6 ± 0.5 nm (Figure 1B).

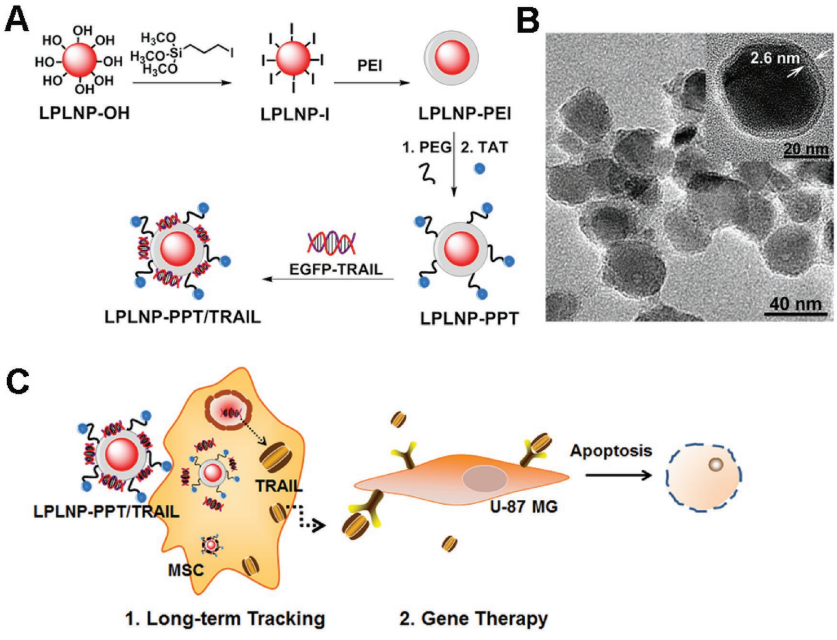

Figure 1. Surface modification and morphology of the LPLNP-PPT. A) Schematic representation of surface modification. B) Transmission electron microscopy image of the LPLNP-PPT. C) Schematic representation of cell tracking and gene therapy.

The surface modification was confirmed by thermogravimetric analysis (TGA), Fourier transform infrared (FT-IR) spectroscopy, and Raman spectroscopy. The Raman spectra of LPLNP-I show a typical C—I stretching vibration at 550 cm^{-1}. In contrast, hydroxylated LPLNP (LPLNP-OH) had no obvious stretching bands (Figure S1A, Supporting Information). The FT-IR spectra of LPLNP-I gave strong the stretching bands of $-CH_2-$ (2924 and 2857 cm^{-1}) and the absorption bands of O—Si—O (1101 and 1047 cm^{-1}), indicating iodine was successfully introduced to LPLNP. The FT-IR spectra of LPLNP-PEI had an obvious stretching band of C—N (1406 cm^{-1}) as a result of successful PEI modification. The final synthesized LPLNP-PPT had a new symmetric C—O—C stretching band (954 cm^{-1}) and C=O stretching band (1739 cm^{-1}) (Figure S1B, Supporting Information). These results show the successful surface modification with PEG and TAT peptide. TGA shows obvious weight losses of 5.9% and 10.9% for LPLNP-PEI and LPLNP-PPT, respectively (Figure S1C, Supporting Information), indicating the pyrolysis of the modified PEI, PEG, and TAT peptide.

Zeta potential and size distribution are key factors for plasmid DNA delivery and pharmacokinetics.[3] LPLNP-OH exhibited a negative zeta potential value of –41.7 ± 1.1 mV. While PEI coating caused a manifest opposite shift, the zeta potential changed from –31.3 to +45.7 mV. The final zeta potential still remained positively charged (+42.1 ± 0.7 mV) after PEGylation and TAT peptide grafting, which is important for binding negatively charged plasmid DNA (Figure S2A, Supporting Information). The hydrodynamic size changed from 52.9 to 122.4 nm with the gradual modification (Figure S2B, Supporting Information).

The positively charged LPLNP-PPT was then loaded with EGFP-TARIL plasmid DNA through electrostatic adsorption. The synthesized LPLNP-PPT/TRAIL composite was used to track the long-term migration of MSC in combination with plasmid DNA transfection. The therapeutic TRAIL ligand expressed from LPLNP-PPT/TRAIL engineered MSC caused apoptosis in glioblastoma U-87 MG cells via interaction with the death receptors (Figure 1C).

2.2. Persistent Luminescence and Plasmid Binding Properties of LPLNP-PPT

The persistent luminescence properties of LPLNP were evaluated after surface modification and plasmid DNA binding. The persistent luminescence excitation, emission, and intensity of LPLNP-PPT and LPLNP-PPT/TRAIL did not change obviously in comparison with those of LPLNP-OH (Figure S3, Supporting Information; **Figure 2**A,B). Good stability is important for biomedical applications. Therefore, we also studied the hydrodynamic size distribution of the LPLNP-PPT and LPLNP-PPT/TRAIL after 24 h incubation in PBS or cell culture medium. No obvious differences were seen, indicating the high

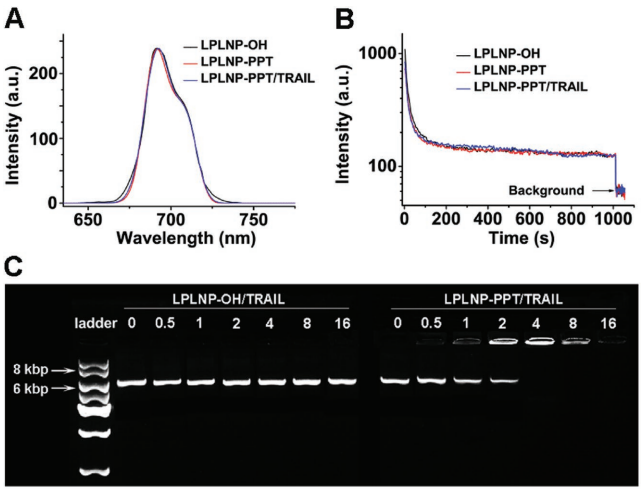

Figure 2. Persistent luminescence and plasmid binding properties of the LPLNP-PPT. A) Emission spectra of the LPLNP-OH, LPLNP-PPT, and LPLNP-PPT/TRAIL (λ_{ex} = 254 nm). B) Persistent luminescence decay curve of the LPLNP-OH, LPLNP-PPT, and LPLNP-PPT/TRAIL, monitored at 694 nm after 5 min UV lamp irradiation. The original reaction weights of LPLNP-OH in LPLNP-OH, LPLNP-PPT, and LPLNP-PPT/TRAIL samples were equal. C) Gel retardation assay of LPLNP-OH/TRAIL and LPLNP-PPT/TRAIL complexes at various weight ratios of nanoparticles to plasmid EGFP-TRAIL.

stability of the LPLNP-PPT and LPLNP-PPT/TRAIL (Figure S4, Supporting Information). To evaluate the capability of LPLNP-PPT for deep brain tissue imaging in vivo, we stereotactically injected LPLNP-PPT (20 μg) into the mouse brain (5 mm depth from dura). Manifest persistent luminescence signals of LPLNP-PPT were visualized. Although the persistent luminescence is getting weak after 2 h, it is recoverable with a red LED excitation (Figure S5, Supporting Information). All these results show the outstanding advantages of deep tissue penetrable and stable persistent luminescence of LPLNP-PPT for in vivo deep brain tissue imaging.

The plasmid DNA binding capacity of LPLNP-PPT was tested by the gel retardation assay. In this assay, the bound DNA remained in the loading wells, while the unbound plasmid DNA freely migrated down the gel. The plasmid DNA was completely retained at LPLNP-PPT/plasmid weight ratio of 4:1. Above that, the visualized DNA in the wells decreased due to the protection from staining by Gel-Red. Importantly, there was no DNA retention in LPLNP-OH/TRAIL complex even in high quantity of LPLNP-OH (Figure 2C). The result confirms that positively charged LPLNP-PPT can efficiently load plasmid DNA.

2.3. Toxicity Study and In Vitro Gene Transfection

The cytotoxicity of LPLNP-PPT was evaluated on MSC, 293T, and U-87 MG cell lines. The viability remains >85% even at the highest dose tested (100 μg mL^{-1}), indicating low cytotoxicity of LPLNP-PPT for multiple cell lines (Figure S6A, Supporting Information). The cytotoxicity of LPLNP-PPT/TRAIL composite on MSC was then studied before cell tracking and gene transfection. MSC was treated with various weight ratios of LPLNP-PPT/TRAIL composite for 48 h. No obvious toxicity was seen with the tested composites (Figure S6B, Supporting Information). These data suggest that LPLNP-PPT/TRAIL labeling has low toxicity on MSC, which can be used for further gene transfection.

MSC has the nature ability to differentiate into various specialized cells. To investigate whether LPLNP-PPT or LPLNP-PPT/TRAIL labeling affects the nature differentiation of MSC, we incubated the labeled MSC with aipogenic, chondrogenic, or osteogenic induction media. Both LPLNP-PPT and LPLNP-PPT/TRAIL labeled MSC had no significant stain difference from normal MSC (Figure S7, Supporting Information). This result shows that labeling of LPLNP-PPT or LPLNP-PPT/TRAIL did not interfere with the differentiation capacity of MSC.

To achieve in vivo gene therapy and cell tracking, we tested the in vivo toxicity of LPLNP-PPT, LPLNP-PPT/TRAIL composite, and LPLNP-PPT/TRAIL labeled MSC. The histological studies of brain and main organs from LPLNP-PPT, LPLNP-PPT/TRAIL composite, or LPLNP-PPT/TRAIL labeled MSC preinjected mice did not show any lesions or damages to tissues (Figure S8, Supporting Information), showing the safety and biocompatibility of LPLNP-PPT, which are necessary for gene delivery and cell tracking.

Plasmid EGFP-TRAIL used here encodes green fluorescence protein (GFP) and therapeutic TRAIL. To evaluate the successful gene transfection of LPLNP-PPT/TRAIL composite, MSC was incubated with the LPLNP-PPT/TRAIL for 12 h. After another 48 h incubation in the fresh culture medium, the fluorescence microscopy images show GFP expression, indicating the successful EGFP-TRAIL transfection in MSC. Moreover, the persistent luminescence signal of LPLNP-PPT was observed in the MSC cytoplasm obviously (Figure S9, Supporting Information). The encoded TRAIL ligand was measured by an enzyme-linked immunosorbent assay (ELISA) (Figure S10, Supporting Information). LPLNP-PPT/TRAIL label MSC produced about 24 pg of TRAIL in the conditioned culture medium (500 μL). These results suggest that LPLNP-PPT could efficiently deliver therapeutic genes into MSC and label MSC for long-term tracking.

2.4. Long-Term Tracking for MSC Homing to GBM

The nature tumor-targeting capacity of MSC is one of the most advantageous characteristics in MSC-based cancer gene therapy.[5] To investigate whether LPLNP-PPT labeling could efficiently track migration of MSC in vitro, we co-cultured LPLNP-PPT labeled MSC and U-87 MG with a 500 μm gap between two cell lines. The real-time luminescence and fluorescence motion analysis shows that LPLNP-PPT labeled MSC migrated rapidly toward U-87 MG, covered the gap, and reached the U-87 MG side in 36 h (**Figure 3**; Movie S1, Supporting Information). These results suggest that LPLNP-PPT labeled MSC maintains tumor-targeting potential and LPLNP-PPT could track the tumor homing of MSC in vitro during the whole migration process.

We then studied the LPLNP-PPT labeled MSC migration to solid GBM in vivo. U-87 MG cells were implanted in the left

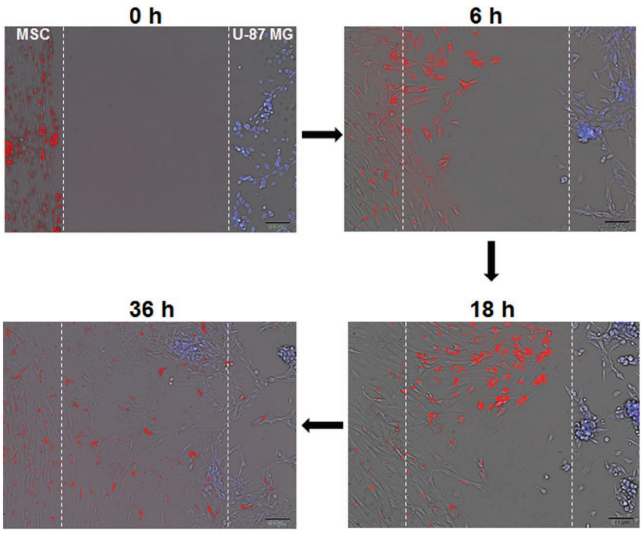

Figure 3. In vitro migration of LPLNP-PPT labeled MSC toward U-87 MG. The persistent luminescence signals (red) of the LPLNP-PPT labeled MSC were captured after 1-min red LED excitation. U-87 MG cells were stained with DAPI (blue). Scale bar: 100 µm.

frontal lobe of mice. Three days later, LPLNP-PPT labeled MSC was injected in the contralateral hemisphere (3 mm deep). In vivo persistent luminescence imaging was studied for three weeks after injection. We found that LPLNP-PPT labeled MSC migrated to GBM across the corpus callosum. On the contrary, no obvious MSC migration was seen in non-tumor-bearing mouse (**Figure 4**A). The natural tumor affinity of MSC likely resulted from chemokines in the tumor microenvironment, such as growth factors.[24] Furthermore, the microscopy images of the sections of tumor tissue taken three weeks

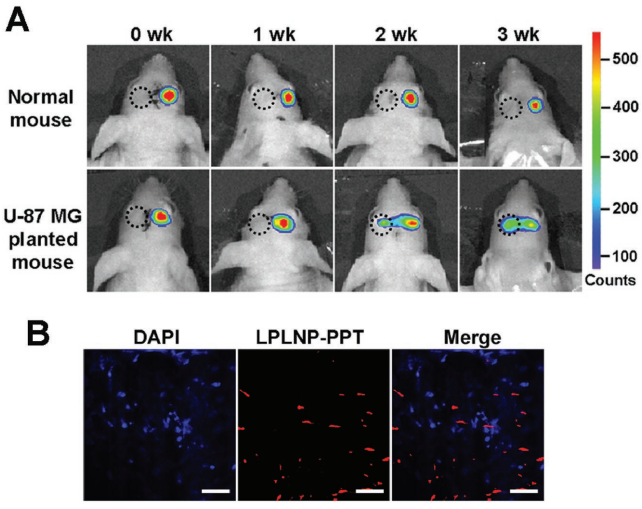

Figure 4. LPLNP-PPT labeled MSC home to GBM. A) In vivo migration study of LPLNP-PPT labeled MSC. B) Persistent luminescence and fluorescence images of the brain tumor slice from GBM bearing mouse. The brain tumor tissues were collected after planting with the LPLNP-PPT labeled MSC in the contralateral hemisphere for three weeks. Cell nuclei were stained by 4′,6-diamidino-2-phenylindole (DAPI) (blue). Red colors represent persistent luminescence signals of LPLNP-PPT. Scale bar: 50 µm.

postimplantation reveal the signals of persistent luminescence from LPLNP-PPT labeled MSC (Figure 4B). The above observations show that LPLNP-PPT labeled MSC possess manifest tumor-homing capacity in vivo. Labeling of LPLNP-PPT could achieve long-term tracking of MSC in deep brain tissue.

2.5. In Vitro and In Vivo Therapeutic Efficacy Study

The in vitro therapeutic efficacy of LPLNP-PPT/TRAIL engineered MSC on U-87 MG cells was evaluated. U-87 MG cells were pretreated with conditioned media collected from untreated MSC, LPLNP-PPT labeled MSC, LPLNP-PPT/GFP labeled MSC, or LPLNP-PPT/TRAIL labeled MSC. Then, the apoptosis degree in U-87 MG cells was evaluated with Annexin V-FITC and PI double staining kit. The fluorescence microscopy images show that only medium from LPLNP-PPT/TRAIL engineered MSC caused numerous positive staining of PI and Annexin V-FITC, in comparison with that of untreated MSC, LPLNP-PPT labeled MSC, or LPLNP-PPT/GFP labeled MSC media (**Figure 5**). The optical images also show that the culture medium treated U-87 MG cells from LPLNP-PPT/TRAIL engineered MSC lost the normal cell morphologies, indicating the dramatic toxicity caused by TRAIL-based gene therapy. Additionally, the cell viability of U-87 MG after treatments was studied. The viability of U-87 MG cells treated with medium from LPLNP-PPT/TRAIL engineered MSC decreased to 52%, while other treatments show no obvious toxicity on U-87 MG tumor cells (Figure S11, Supporting Information), which is in good agreement with the apoptosis staining results. These results confirm that TRAIL expressed by LPLNP-PPT/TRAIL engineered MSC efficiently caused apoptosis in the cells of U-87 MG.

To investigate whether the therapeutic efficacy of LPLNP-PPT/TRAIL engineered MSC also occurs in vivo, we preestablished U-87 MG brain tumor model. Three days later, the tumor-baring mice were divided into three groups and respectively treated with intratumoral injection of PBS, normal MSC, and LPLNP-PPT/TRAIL engineered MSC. The histology study (**Figure 6**A) and tumor volume calculation (Figure 6B) show that the brain tumor growth was extremely inhibited by LPLNP-PPT/TRAIL engineered MSC. Three weeks later, the tumor length was less than 1 mm with LPLNP-PPT/TRAIL engineered MSC treatment whereas the tumor length was about 4 mm in PBS and normal MSC treated mice.

Meanwhile, to evaluate the in vivo apoptosis-inducing capability of TRAIL expressed by LPLNP-PPT/TRAIL engineered MSC, the tumor tissue sections were performed TUNEL staining. LPLNP-PPT/TRAIL engineered MSC caused more apoptosis than that of PBS or normal MSC, as shown in numerous TUNEL positive stained tumor cells (Figure 6C). These results indicate that LPLNP-PPT/TRAIL engineered MSC induced tumor cell apoptosis in vivo.

3. Conclusion

In conclusion, we have developed the core–shell nanostructured LPLNP-PPT for effective gene delivery and tracking of

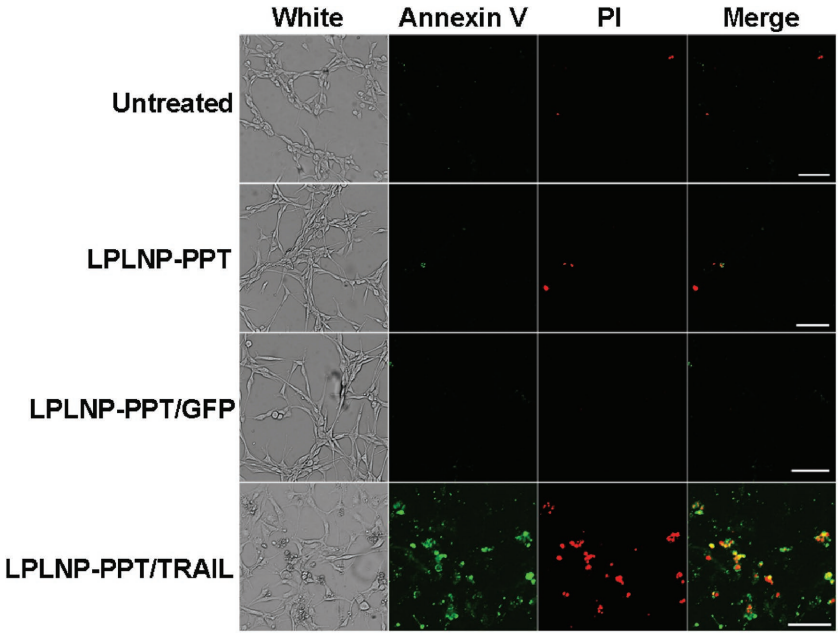

Figure 5. In vitro gene therapy induces apoptosis in U-87 MG cells. U-87 MG cells were incubated with conditioned media collected from untreated MSC, LPLNP-PPT labeled MSC, LPLNP-PPT/GFP labeled MSC, or LPLNP-PPT/TRAIL labeled MSC. Scale bar: 100 µm.

MSC, without affecting their natural proliferation, differentiation, and tumouritropic migration capabilities. The positively charged LPLNP-PPT shows high plasmid loading ability, NIR-emitted long persistent luminescence, and low toxicity. Such promising features make LPLNP-PPT a dual-functional composite for tracking and gene delivery in the meantime. LPLNP-PPT/TRAIL engineered MSC can migrate to the cells of glioblastoma U-87 MG both in vivo and in culture. The encoded anticancer TRAIL ligand from LPLNP-PPT/TRAIL engineered MSC could induce apoptosis and suppress progression of the glioblastoma. LPLNP-PPT/TRAIL engineered MSC possess diagnostic and therapeutic functionalities, and will open great interests for clinical applications in stem-cell-based therapy. The controllable integration of LPLNP with other one or more functional components shows great potential for clinical theranostic applications.

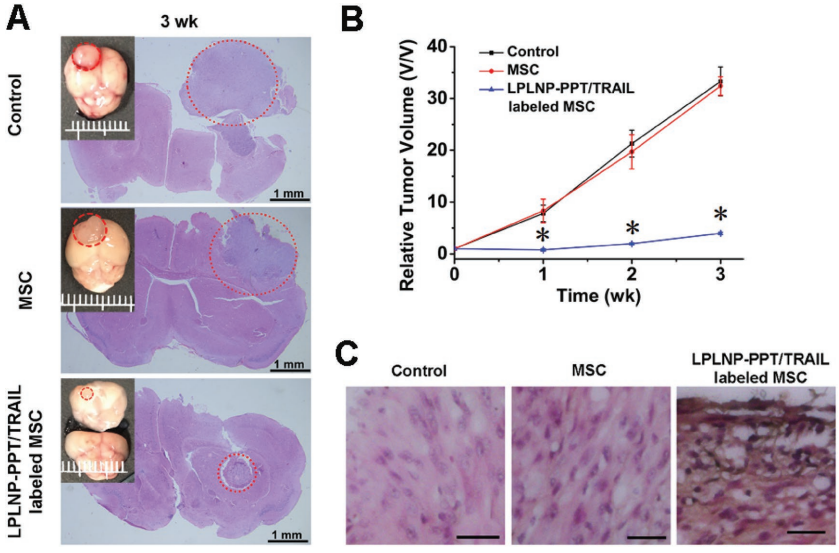

Figure 6. In vivo therapeutic efficacy of LPLNP-PPT/TRAIL labeled MSC. A) Histology study of brains from mice respectively pretreated with phosphate buffer saline (PBS), MSC, and LPLNP-PPT/TRAIL labeled MSC. B) Calculation of the relative brain tumor volumes. C) Terminal deoxynucleotidyl transferase-mediated dUTP nick-end labeling (TUNEL) study revealed significant apoptosis in the brain tumors from LPLNP-PPT/TRAIL labeled MSC treated mouse. Scale bar: 20 µm; $^*P < 0.05$.

4. Experimental Section

Chemicals and Materials: All reagents were bought from Aladdin (Shanghai, China) unless otherwise stated. Branched PEI (M_w, 10 kDa) was purchased from Alfa Aesar (Shanghai, China). Mal-NH-PEG-CH_2CH_2COONHS (average M_w, 4000 Da) was obtained from Biomatrik Inc. (Zhejiang, China). TAT peptide CALNNAGRKKRRQRRR (M_w, 1983.35 Da) was purchased from ChinaPeptides Co. Ltd. (Shanghai, China). Annexin V-FITC Apoptosis Detection Kit was from GEN-VIEW SCIENTIFIC Inc. (Calimesa, USA). Colorimetric TUNEL Apoptosis Assay Kit was obtained from Beyotime (Shanghai, China). 3-(4,5-dimethylthiazol-2-yl)-2,5-diphenyktetrazolium bromide (MTT) was purchased from Sigma-Aldrich Co. LLC (Shanghai, China). The plasmid pEGFP-TRAIL and EGFP were purchased from Changsha Yingrun Biotechnology Co. Ltd. (Changsha, China).

Characterization: Luminescence spectra were collected on the F-4500 spectrofluorometer (Hitachi, Japan). FT-IR spectra were collected on the Nicolet 6700 spectrometer (Thermo Fisher Scientific, USA). Raman spectra were acquired on the InVia Raman microscope system (Renishaw, UK). TEM experiments were conducted on the Tecnai G2 F20 transmission electron microscope (FEI, USA). TGA data were acquired on the TG209 thermal analyzer (Netzsch, Germany) in N_2 atmosphere. Zeta potential and dynamic light scattering analysis were carried out on the Zetasizer Nano-ZS (Malvern, UK). The microscopic luminescence images were acquired with the inverted fluorescence microscope (AF7000, Leica, Germany) fitted with the EMCCD camera (Andor, UK). Persistent luminescence was collected on the IVIS Imaging System (PerkinElmer, USA). Mice were pre-excited with the red LED light of 650 nm (5000 lm) before capturing persistent luminescence signals.

Synthesis and Surface Modification of LPLNP: LPLNP with composition of $Zn_{1.1}Ga_{1.8}Ge_{0.1}O_4$: 0.5%$Cr^{3+}$,0.5%$Eu^{3+}$ was synthesized as described previously.[20] After reacting with NaOH (5×10^{-3} M) solution, the LPLNP-OH was obtained.

LPLNP-I was obtained by adding 3-iodopropyltrimethoxysilan (250 µL) to a suspension of LPLNP-OH (50 mg) in toluene (10 mL). Ultrasonification and vigorous stirring were applied to the reaction mixture at 80 °C for 12 h, then the mixture was centrifuged and the obtained LPLNP-I was washed with methanol to remove excessive 3-iodopropyltrimethoxysilan.

LPLNP-PEI was prepared by adding PEI (200 mg) and triethylamine (20 µL) to a suspension of LPLNP-I (25 mg) in *N*,*N*-dimethyleformamide

(DMF) (10 mL). Ultrasonification and vigorous stirring were applied to the reaction mixture at 50 °C for 8 h, then the resulting LPLNP-PEI was collected by centrifugation with subsequent DMF and methanol washing.

To conjugate PEG and TAT peptide, LPLNP-PEI (20 mg) was first reacted with Mal-NH-PEG-CH_2CH_2COONHS (20 mg) in DMF (2 mL) containing triethylamine (4 µL) for 6 h. Then, TAT peptide (10 mg) in PBS (10 mL) was added, and stirred in dark at room temperature overnight. The reaction mixture was centrifuged and washed with H_2O and the resulting LPLNP-PPT was freeze dried.

Cell Culture: Human bone marrow MSC (Cyagen Biosciences, Guangzhou, China) was cultured and then expanded in a 10-cm^2 plate in the complete growth medium (Cyagen Biosciences, China) at 37 °C in 5% CO_2. the cells of U-87 MG and 293T (Procell, Wuhan, China) were cultured in MEM-EBSS (MEM Eagles with Earle's Balanced Salts) or RPMI 1640 medium supplemented with 10% fetal bovine serum and 100 U mL^{-1} of penicillin–streptomycin at 37 °C in 5% CO_2.

Animal Model: Balb/c nude male mice with five-week-old (HFK Bioscience Co., Beijing, China) were anesthetized with intraperitoneally administered pentobarbital in all animal procedures. All experiments for animals were performed under the instructions of the Tianjin Committee of Use and Care of Laboratory Animals.

Glioma mouse model was established by injecting U-87 MG into the brain. U-87 MG was collected by trypsinization, washed and resuspended in PBS (1×10^5 cells in PBS (4 µL)). The cells were injected stereotactically to the left frontal lobe (2.0 mm lateral, 0.5 mm caudal to bregma, and 3 mm depth from dura) of mice.

In Vivo Deep Brain Tissue Imaging: 5 min UV lamp preirradiation was applied to LPLNP-PPT (20 µg) in PBS (10 µL) before stereotactical injection to the frontal lobe (5 mm depth from dura) of mouse. Persistent luminescence decay was collected to 2 h. On 3, 4, and 5 h after injection, the mouse was received 1-min LED light excitation before acquiring the persistent luminescence.

LPLNP-PPT/TRAIL Formation and Gel Retardation Assay: Plasmid DNA (EGFP-TRAIL, 150 ng) was incubated with various amount of LPLNP-PPT corresponding to the weight ratios (LPLNP-PPT: EGFP-TRAIL = 0, 0.5, 1, 2, 4, 8, 16) in the 4,2-hydroxyethyl-1-piperazineethanesulfonic acid (HEPES) buffer (20×10^{-3} M, pH 7.4). The mixture was vortexed and incubated at room temperature for 1.5 h before they were analyzed by 1% agarose gel (containing Gel-Red) electrophoresis in a tris-acetate-EDTA buffer at 100 mV for 1.5 h. Images were obtained on C150 Azure Biosystems. Negatively charged LPLNP-OH nanoparticles were used as controls following the same procedures.

Cytotoxicity Assay (MTT): To determine the toxicity of LPLNP-PPT against multiple cell types, the cells MSC, 293T, and U-87 MG were seeded in the 96-well plate with 5×10^3 cells per well and incubated overnight in MSC complete growth medium, RPMI 1640 or MEM culture medium, respectively. The cells were washed with PBS once and then incubated in fresh culture medium containing various amounts of LPLNP-PPT (0, 50, 100 µg mL^{-1}) for 48 h. After washing with PBS twice, the cells were received MTT analysis as described previously.[20]

The cytotoxicity of LPLNP-PPT/TRAIL composite was evaluated in MSC before transfection. MSC was seeded in the 96-well plate (5×10^3 cells per well) and cultured in complete growth medium overnight. The different weight ratios of LPLNP-PPT/TRAIL composite were prepared for 1 h prior to cellular incubation for 48 h. The supernatants were removed, and PBS was then used to wash the cells for subsequent MTT analysis.

Cell Transfection: MSC was seeded in the 6-well plates (5×10^5 cells per well) and incubated overnight before transfection. LPLNP-PPT/TRAIL composite (wt:wt = 4:1, 2 µg of EGFP-TRAIL in each well) was added into MSC culture medium, then incubated the cells for 12 h. PBS was used to wash the cells twice for subsequent cell incubation in fresh culture medium for another 48 h before imaging on an inverted microscope. 1 min LED light pre-excitation was applied to the cells before acquiring luminescence images.

ELISA to Detect TRAIL Expression: The concentration of expressed TRAIL in the condition culture media from untreated MSC, LPLNP-PPT labeled MSC, and LPLNP-PPT/TRAIL labeled MSC was detected with Quantikine Human TRAIL Immunoassay (R&D Systems) following the manufacturer's protocols.

In Vitro Differentiation Study of MSC: The effect of LPLNP-PPT or LPLNP-PPT/TRAIL composite on the differentiation capability of MSC was studied. MSC was plated in 12-well plates (5×10^4 cells per well), then preincubated with free medium, LPLNP-PPT containing medium, or LPLNP-PPT/TRAIL containing medium for 48 h. To induce adipogenic or osteogenic differentiation, MSC was incubated with adipogenic or osteogenic induction medium (BIOWIT Technologies, China), respectively. The induction media were changed every two days in two weeks. Chondrogenic differentiation was performed by incubating the cells in chondrogenic induction medium which was refreshed every three days in three weeks. Adipogenic, chondrogenic, and osteogenic differentiation were then evaluated by staining with oil-red O, alizarin red S, and toluidine blue, respectively.

Histology Study: LPLNP-PPT (800 µg), LPLNP-PPT/TRAIL (800 µg), LPLNP-PPT/TRAIL labeled MSC (10^6) in PBS (100 µL), or free PBS were injected intravenously into healthy mice ($n = 4$). The studied mice were sacrificed 14 days later and the major organs (heart, liver, spleen, lung, kidney) and the brain were collected. The tissues were fixed and embedded into paraffin, sectioned for 8-µm thick. The sections were stained with hematoxylin–eosin and imaged on optical microscopy. The images were read by an experienced veterinary pathologist.

In Vitro Migration Study of MSC: MSC was seeded in the left microculture inserts using two-chamber cell culture insert (Ibidi, Germany) in 35 mm-glass bottom confocal dish. U-87 MG was seeded into the right well. MSC was labeled with LPLNP-PPT for 12 h, while U87-MG was stained with DAPI for 1 h. After the cell culture insert was removed, the cells were imaged at 10× magnification every 30 min in a live cell imaging system. Images were used to generate a movie using PPT converter.

In Vivo Migration Study of MSC: Tumor bearing mice were performed by intracranial injection of U-87 MG cells. Non-tumor-bearing mice were used as controls. Three days later, LPLNP-PPT labeled MSC (10^5) in PBS (4 µL) was planted in the contralateral hemisphere of the tumor bearing mice or healthy mice. The NIR persistent luminescence signals were acquired every week. The glioma tissue slices from mouse planted with LPLNP-PPT labeled MSC for three weeks were fixed for subsequent DAPI staining. The luminescence images were then acquired on the inverted microscope.

In Vitro Apoptotic Assay: The cells U-87 MG were seeded in the 24-well plate (5×10^4 cells per well). MSC cells were incubated with LPLNP-PPT, LPLNP-PPT/GFP composite, or LPLNP-PPT/TRAIL composite for 12 h. After washing twice with PBS, the cells were incubated in fresh culture medium for another five days. The supernatants from different treated MSC were collected and incubated U-87 MG cells for 48 h, respectively. Thereafter, the U-87 MG cells were fixed and stained with the Annexin V-FITC/PI Apoptosis Detection kit according to the manufacturer's protocol. The viability of U-87 MG was also studied by the MTT assay.

In Vivo Therapeutic Effect of LPLNP-PPT/TRAIL Labeled MSC on Glioblastoma: The brain tumor bearing mice were randomly divided into three groups ($n = 8$). Three days later, the mice were respectively injected with PBS, normal MSC, and LPLNP-PPT/TRAIL labeled MSC into the tumor. Sacrification of the mice was carried out three weeks later. The brains were acquired for histology study and tumor volume calculation. The brain sections were also performed TUNEL assay following the manufacturer's protocol. A digital caliper was used to measure the length and width of the brain tumors to calculate the tumor volume based on length × $width^2/2$.

Supporting Information

Supporting Information is available from the Wiley Online Library or from the author.

Acknowledgements

The authors appreciate the financial support from the National Natural Science Foundation of China (Grant Nos. 21435001 and 21275079).

Received: September 26, 2016
Revised: November 13, 2016
Published online: February 6, 2017

[1] T. M. Kauer, J.-L. Figueiredo, S. Hingtgen, K. Shah, *Nat. Neurosci.* **2011**, *15*, 197.
[2] L. Zeng, L. Zou, H. Yu, X. He, H. Cao, Z. Zhang, Q. Yin, P. Zhang, W. Gu, L. Chen, Y. Li, *Adv. Funct. Mater.* **2016**, *26*, 4201.
[3] K. Wang, F. M. Kievit, M. Jeon, J. R. Silber, R. G. Ellenbogen, M. Zhang, *Adv. Healthcare Mater.* **2015**, *4*, 2719.
[4] G. Tian, X. Zhang, Z. Gu, Y. Zhao, *Adv. Mater.* **2015**, *27*, 7692.
[5] J. R. Bagó, A. Alfonso-Pecchio, O. Okolie, R. Dumitru, A. Rinkenbaugh, A. S. Baldwin, C. R. Miller, S. T. Magness, S. D. Hingtgen, *Nat. Commun.* **2016**, *7*, 10593.
[6] R. Vankayala, C. L. Kuo, K. Nuthalapati, C. S. Chiang, K. Hwang, *Adv. Funct. Mater.* **2015**, *25*, 5934.
[7] X. Wang, K. Liu, G. Yang, L. Cheng, L. He, Y. Liu, Y. Li, L. Guo, Z. Liu, *Nanoscale* **2014**, *6*, 9198.
[8] Y.-L. Hu, B. Huang, T.-Y. Zhang, P.-H. Miao, G.-P. Tang, Y. Tabata, J.-Q. Gao, *Mol. Pharmaceutics* **2012**, *9*, 2698.
[9] B. Cao, M. Yang, Y. Zhu, X. Qu, C. Mao, *Adv. Mater.* **2014**, *26*, 4627.
[10] R. A. Daniels, H. Turley, F. C. Kimberley, X. S. Liu, J. Mongkolsapaya, P. Ch'En, X. N. Xu, B. Q. Jin, F. Pezzella, G. R. Screaton, *Cell Res.* **2005**, *15*, 430.
[11] S. Kagawa, C. He, J. Gu, P. Koch, S. J. Rha, J. A. Roth, S. A. Curley, L. C. Stephens, B. Fang, *Cancer Res.* **2001**, *61*, 3330.
[12] N. Redjal, Y. Zhu, K. Shah, *Stem Cells* **2015**, *33*, 101.
[13] A. Nakamizo, F. Marini, T. Amano, A. Khan, M. Studeny, J. Gumin, J. Chen, S. Hentschel, G. Vecil, J. Dembinski, M. Andreeff, F. F. Lang, *Cancer Res.* **2005**, *65*, 3307.
[14] M. Cihova, V. Altanerova, C. Altaner, *Mol. Pharmaceutics* **2011**, *8*, 1480.
[15] N. E. Furman, Y. Lupu-Haber, T. Bronshtein, L. Kaneti, N. Letko, E. Weinstein, L. Baruch, M. Machluf, *Nano Lett.* **2013**, *13*, 3248.
[16] P. J. Chen, Y. D. Kang, C. H. Lin, S. Y. Chen, C. H. Hsieh, Y. Y. Chen, C. W. Chiang, W. Lee, C. Y. Hsu, L. D. Liao, C. T. Fan, M. L. Li, W. C. Shyu, *Adv. Mater.* **2015**, *27*, 6488.
[17] M. F. Kircher, S. S. Gambhir, J. Grimm, *Nat. Rev. Clin. Oncol.* **2011**, *8*, 677.
[18] T. Maldiney, A. Bessière, J. Seguin, E. Teston, S. K. Sharma, B. Viana, A. J. J. Bos, P. Dorenbos, M. Bessodes, D. Gourier, D. Scherman, C. Richard, *Nat. Mater.* **2014**, *13*, 418.
[19] Y.-J. Chuang, Z. Zhen, F. Zhang, F. Liu, J. P. Mishra, W. Tang, H. Chen, X. Huang, L. Wang, X. Chen, J. Xie, Z. Pan, *Theranostics* **2014**, *4*, 1112.
[20] S.-Q. Wu, C.-W. Chi, C.-X. Yang, X.-P. Yan, *Anal. Chem.* **2016**, *88*, 4114.
[21] T. Xia, M. Kovochich, M. Liong, H. Meng, S. Kabehie, S. George, J. I. Zink, A. E. Nel, *ACS Nano* **2009**, *3*, 3273.
[22] B. Shah, P. T. Yin, S. Ghoshal, K.-B. Lee, *Angew. Chem. Int. Ed.* **2013**, *52*, 6190.
[23] Y. Liu, J. Du, J.-S. Choi, K.-J. Chen, S. Hou, M. Yan, W.-Y. Lin, K. Chen, T. Ro, G. S. Lipshutz, L. Wu, L. Shi, Y. Lu, H.-R. Tseng, H. Wang, *Angew. Chem. Int. Ed.* **2016**, *55*, 169.
[24] M. F. Corsten, K. Shah, *Lancet Oncol.* **2008**, *9*, 376.